

Supporting information for “Diiron Azamonothiolates via Scission of Dithiadiazacyclooctanes by Iron Carbonyls”

Table of contents:

Variable Temperature ^1H NMR spectra for $\text{S}_2\text{N}^{\text{Me}}_2$ in d_8 -THF	pg 1
FTIR spectra of diiron carbonyl complexes discussed in this report	pg 1
^1H NMR spectrum of $\text{Fe}_2[\text{SCH}_2\text{N}(\text{CH}_3)\text{CH}_2](\text{CO})_6$, $\mathbf{1}^{\text{Me}}$ in CD_2Cl_2	pg 2
^1H - ^1H gCOSY spectrum of $\mathbf{1}^{\text{Me}}$ in CD_2Cl_2	pg 2
^1H - ^{13}C HSQC spectrum of $\mathbf{1}^{\text{Me}}$ in CD_2Cl_2	pg 3
Cyclic Voltammogram of $\mathbf{1}^{\text{Me}}$	Pg 3
Arrhenius plots for stereodynamics of $\mathbf{1}^{\text{Me}}$	pg 4
Variable Temperature ^{13}C NMR spectra of $\mathbf{1}^{\text{Me}}$ in d^8 -toluene.....	pg 4
^{13}C NMR spectra of $\mathbf{1}^{\text{Me}}$ in d^8 -toluene containing an internal standard.....	pg 5
Full ^{13}C NMR spectrum of $\mathbf{1}^{\text{Me}}$ in d^8 -toluene	pg 5
Variable Temperature ^{13}C NMR spectra of $\mathbf{1}^{\text{Me}}$ in CD_2Cl_2	pg 6
^1H NMR spectrum of $\text{Fe}_2[\text{SCH}_2\text{N}(\text{CH}_3)\text{CH}_2](\text{CO})_5\text{PPh}_3$, $\mathbf{3}^{\text{Me}}$ in CD_2Cl_2	pg 6
$^{31}\text{P}\{^1\text{H}\}$ NMR spectrum of crystals of $\mathbf{3}^{\text{Me}}$ in CD_2Cl_2	pg 7
^{13}C NMR spectrum of crystals of $\mathbf{3}^{\text{Me}}$ in CD_2Cl_2	pg 7
^1H NMR spectrum of crystals of $\mathbf{3}^{\text{Me}}$ in CD_2Cl_2 after isomerization.....	pg 8
$^{31}\text{P}\{^1\text{H}\}$ NMR spectrum of crystals of $\mathbf{3}^{\text{Me}}$ in CD_2Cl_2 after isomerization	pg 8
^1H NMR spectrum of $\text{Fe}_2[\text{SCH}_2\text{N}(\text{CH}_3)\text{CH}_2](\text{CO})_5\text{PMe}_3$, $\mathbf{4}^{\text{Me}}$ in CD_2Cl_2	pg 9
Variable Temperature $^{31}\text{P}\{^1\text{H}\}$ NMR spectra of $\mathbf{4}^{\text{Me}}$ in d^8 -toluene	pg 9
Full ^{13}C NMR spectrum of $\mathbf{4}^{\text{Me}}$ in d^8 -toluene	pg 10
^{13}C NMR spectrum of $\mathbf{4}^{\text{Me}}$ in d^8 -toluene at -60 °C highlighting CO region	pg 10
^1H NMR spectrum of $\text{Fe}_2[\text{SCH}_2\text{N}(\text{CH}_3)\text{CH}_2](\text{CO})_4(\text{dppe})$, $\mathbf{5}^{\text{Me}}$ in CD_2Cl_2	pg 11
$^{31}\text{P}\{^1\text{H}\}$ NMR spectrum of $\mathbf{5}^{\text{Me}}$ in CD_2Cl_2	pg 11
^{13}C NMR spectrum of $\mathbf{5}^{\text{Me}}$ in CD_2Cl_2	pg 12

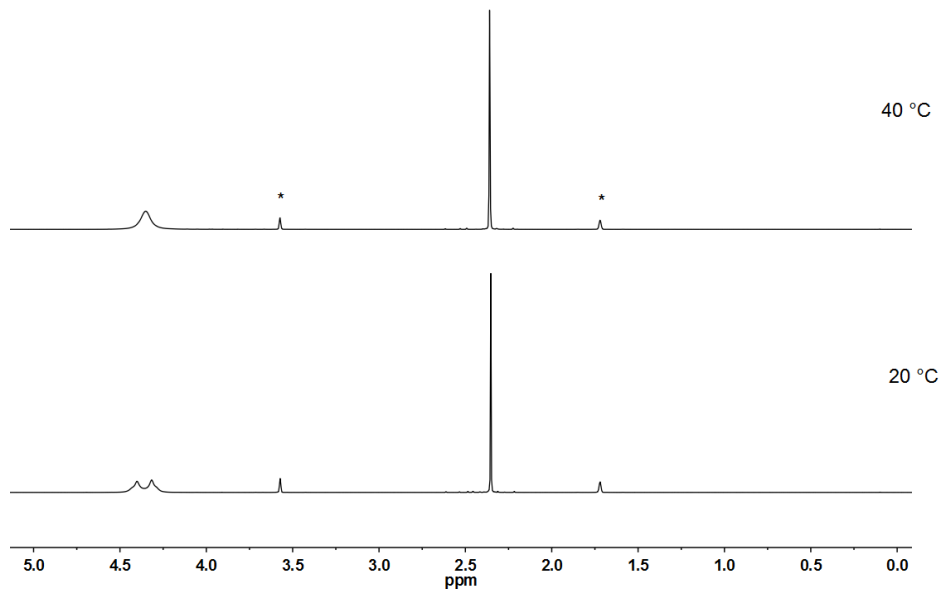


Figure S1: ^1H NMR spectra (500 MHz, $d_8\text{-THF}$) of $\text{S}_2\text{N}^{\text{Me}}_2$ at two temperatures. * Residual solvent. δ 2.44 (s, 6H, NCH_3), 4.24 (d, 4H, NCH_2S), 4.52 (d, 4H, NCH_2S).

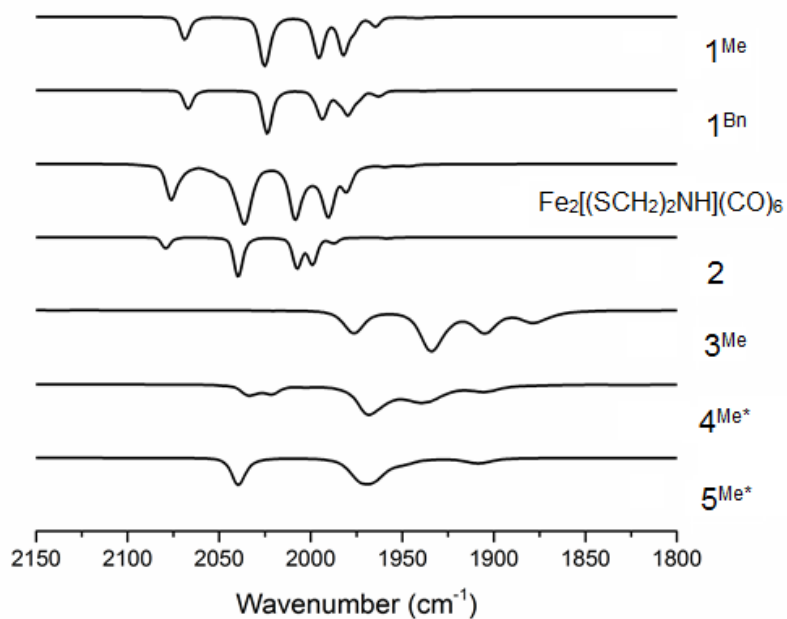


Figure S2. IR spectra of compounds discussed in this report recorded in hexanes.* Recorded on CH_2Cl_2 solutions.

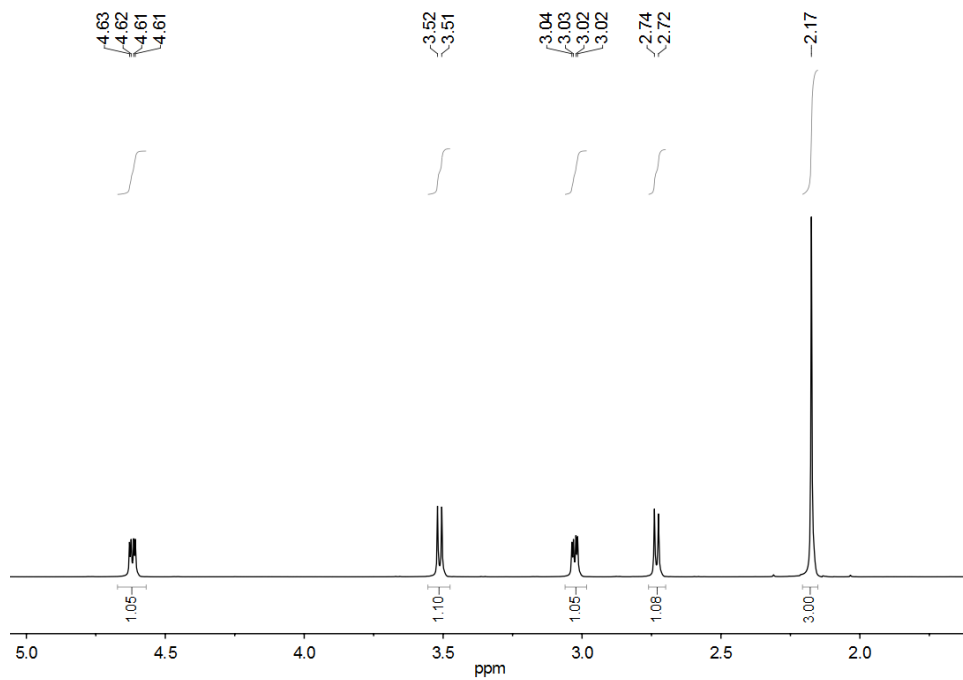


Figure S3. ^1H NMR spectrum (500 MHz, CD_2Cl_2 solution) of $\mathbf{1}^{\text{Me}}$.

Assignments: δ 2.17 (s, 3H, NCH_3), 2.73 (d, 1H, NCH_2Fe), 3.03 (dd, 1H, NCH_2Fe), 3.52 (d, 1H, NCH_2S), 4.63 (dd, 1H, NCH_2S).

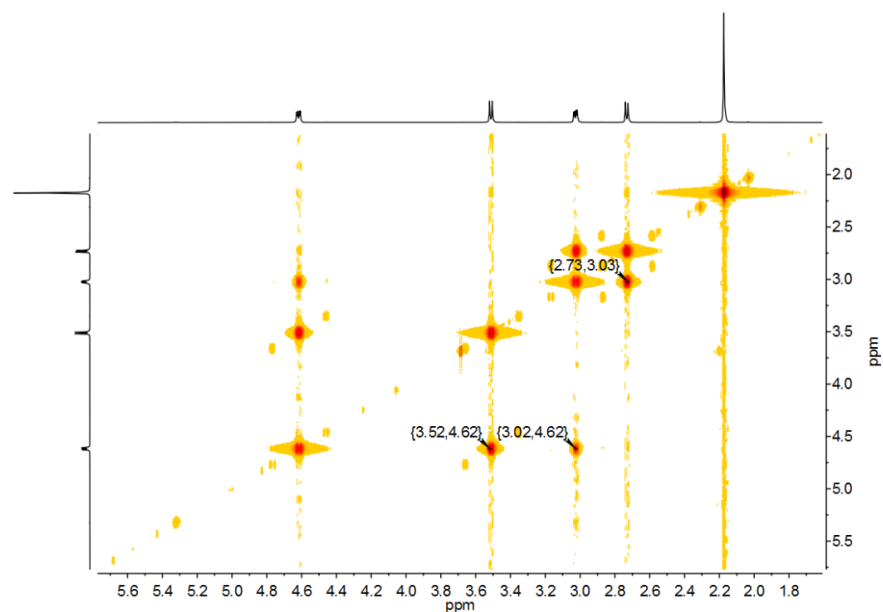


Figure S4. ^1H - ^1H correlation (COSY) NMR spectrum (500 MHz, CD_2Cl_2 solution) of $\mathbf{1}^{\text{Me}}$.

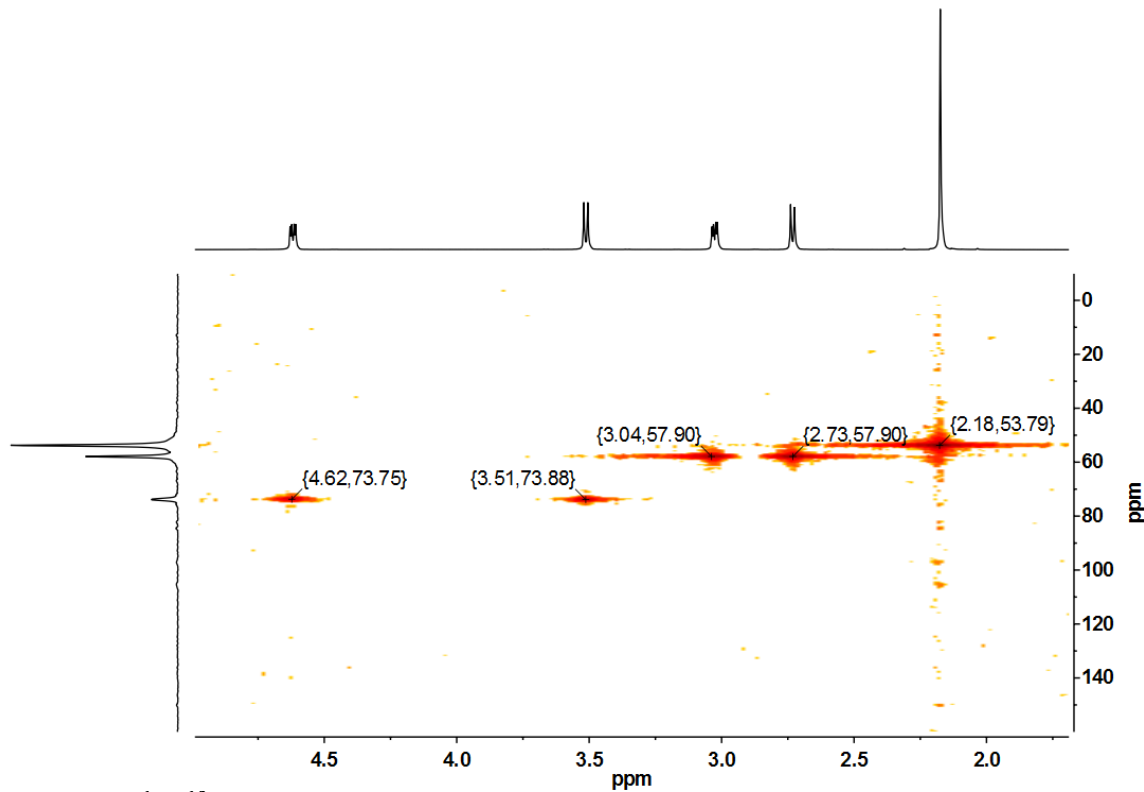


Figure S5. ^1H - ^{13}C heteronuclear single-quantum correlation (HSQC) NMR spectrum (500 MHz, CD_2Cl_2 solution) of $\mathbf{1}^{\text{Me}}$.

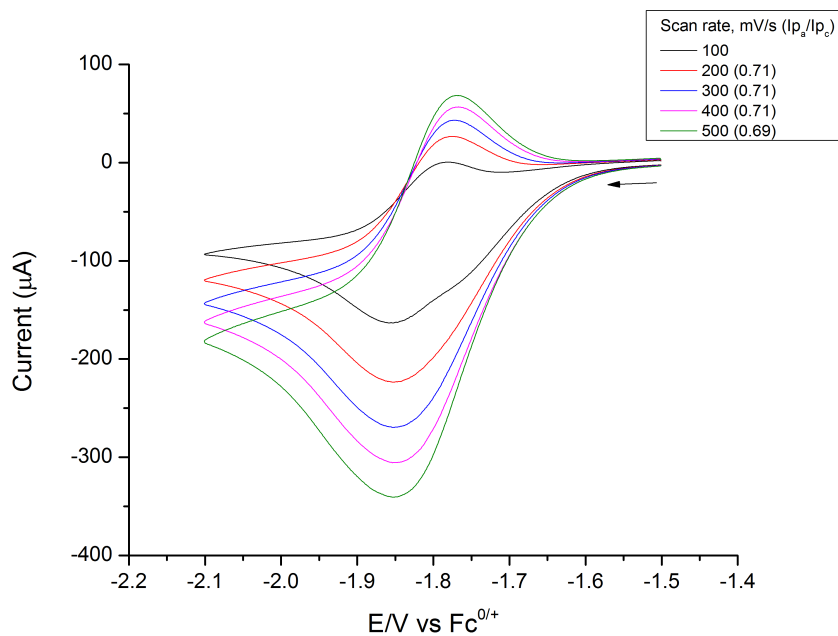


Figure S6. Cyclic Voltammogram of $\mathbf{1}^{\text{Me}}$ at various scan rates. *Conditions:* 3 mM solution in CH_2Cl_2 , 0.1 M NBu_4PF_6 electrolyte; glassy carbon working electrode, Ag/AgCl reference electrode, and Pt wire counter electrode.

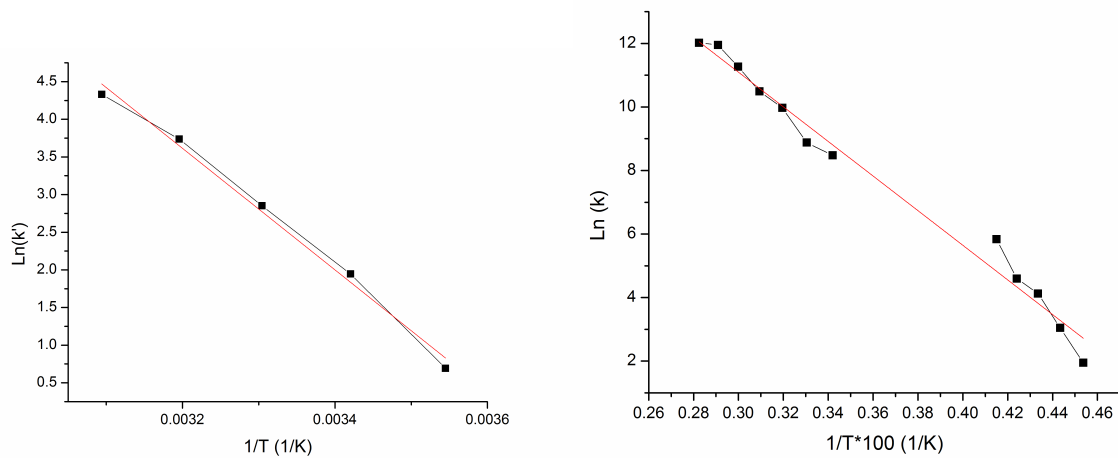


Figure S7. Arrhenius plots for the dynamic processes of $\mathbf{1}^{\text{Me}}$ described by k_{rigid} (left), and $k_{\text{non-rigid}}$ (right).

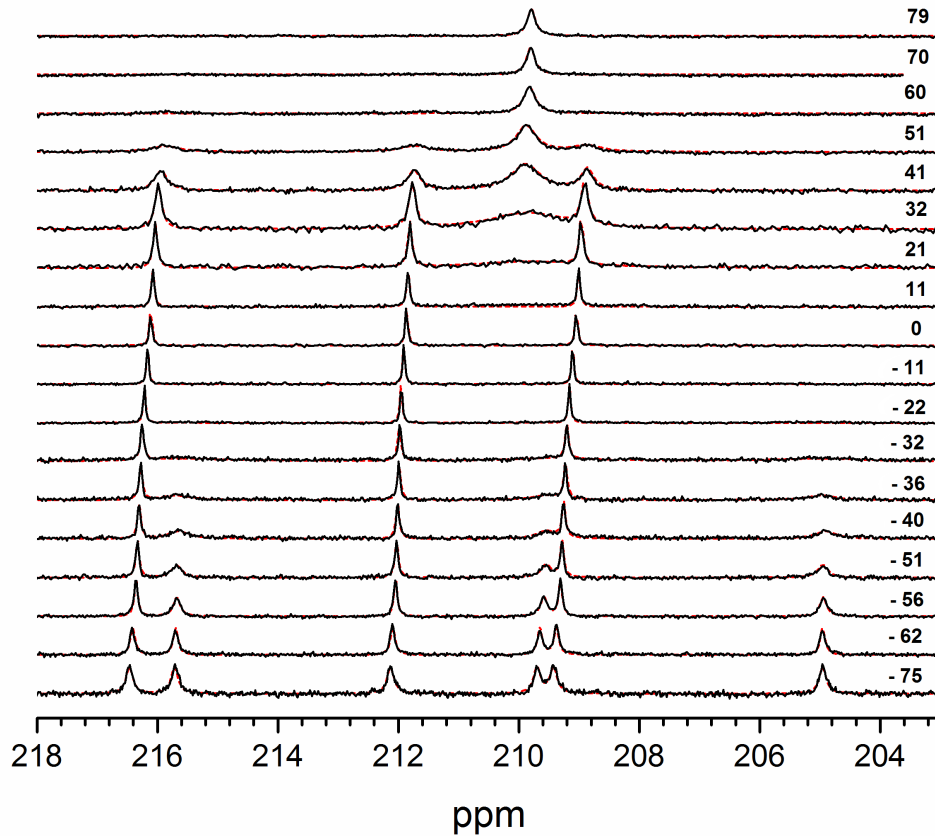


Figure S8: ^{13}C NMR spectra (125.7 MHz, d_8 -toluene solution) of compound $\mathbf{1}^{\text{Me}}$ at various temperatures (black), and NMR simulations (red) at various temperatures ($^{\circ}\text{C}$). Simulations were generated using WIND-NMR software provided by Hans J. Reich, University of Wisconsin.

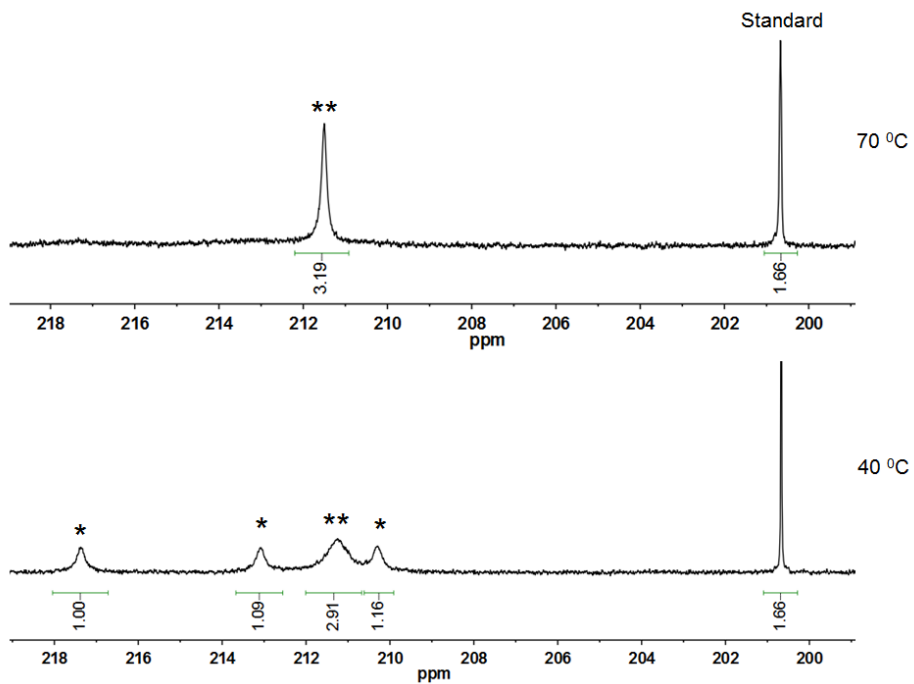


Figure S9. ^{13}C NMR spectra (125.7 MHz, d_8 -toluene solution) of $\mathbf{1}^{\text{Me}}$ at two temperatures with ethylacetooctate as an internal standard. *Rigid, ** Non-rigid.

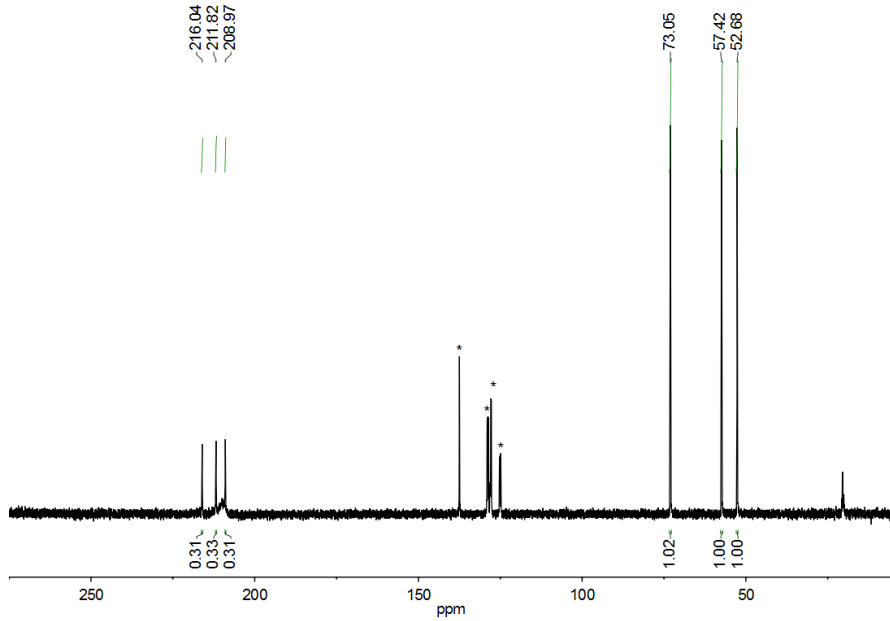


Figure S10. $^{13}\text{C}\{^1\text{H}\}$ NMR spectrum (125.7 MHz, d_8 -toluene solution) of $\mathbf{1}^{\text{Me}}$ at 20 °C. * Residual solvent. *Assignments:* δ 52.7 (s, 1C, NCH_3), 57.4 (s, 1C, NCH_2Fe), 73.1 (s, 1C, NCH_2S).

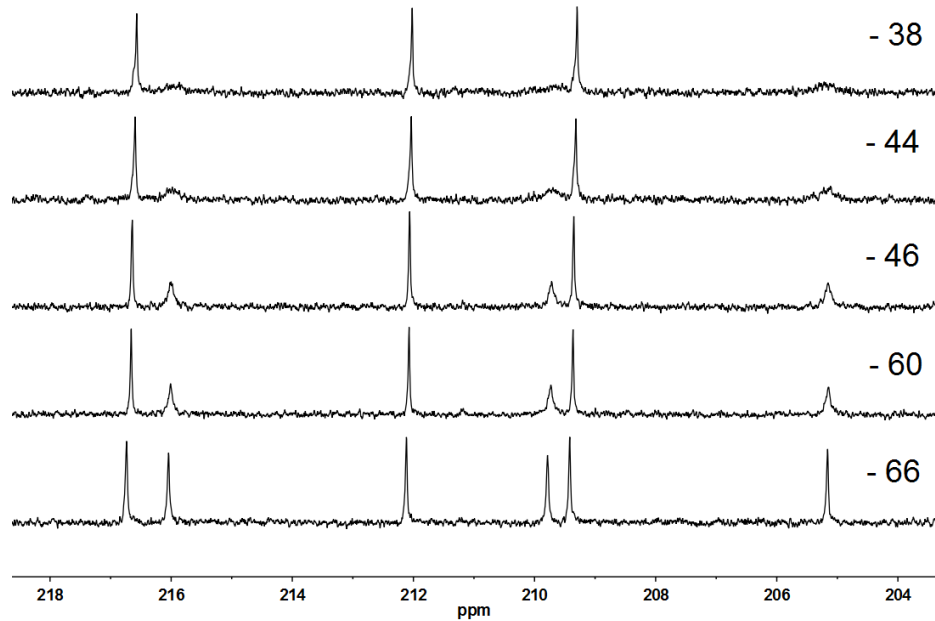


Figure S11. $^{13}\text{C}\{\text{H}\}$ NMR spectra (126 MHz, CD_2Cl_2 solution) of $\mathbf{1}^{\text{Me}}$ recorded at various temperatures.

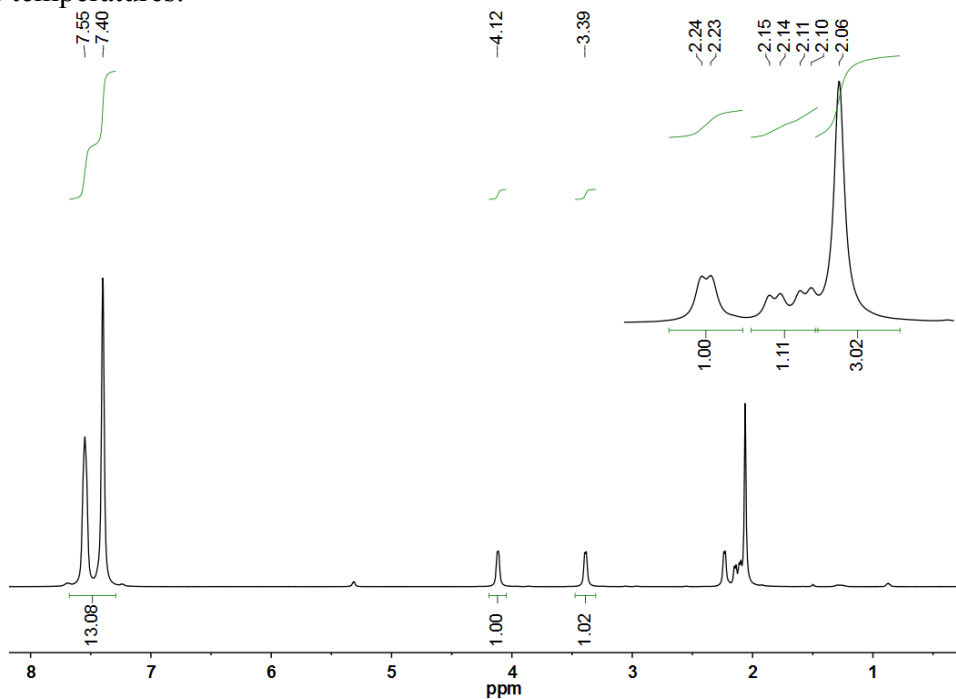


Figure S12. ^1H NMR spectrum of crystals of $\mathbf{3}^{\text{Me}}$ (500 MHz, CD_2Cl_2 solution).

Assignments: δ 2.06 (s, 3H, NCH_3), 2.12 (d, 1H, NCH_2Fe), 2.23 (dd, 1H, NCH_2Fe), 3.39 (d, 1H, NCH_2S), 4.12 (dd, 1H, NCH_2S), 7.40-7.55 (2s, 15H, $\text{P}(\text{C}_6\text{H}_5)_3$).

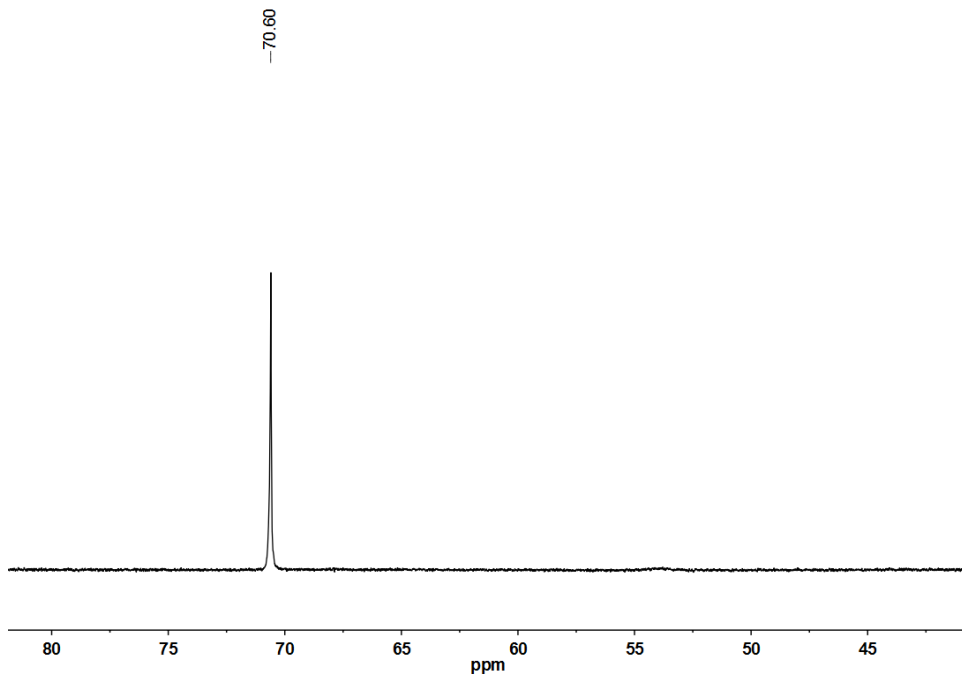


Figure S13. $^{31}\text{P}\{\text{H}\}$ NMR spectrum of crystals of 3^{Me} (202 MHz, CD_2Cl_2 solution). Assignments: δ 70.60 (PPh_3).

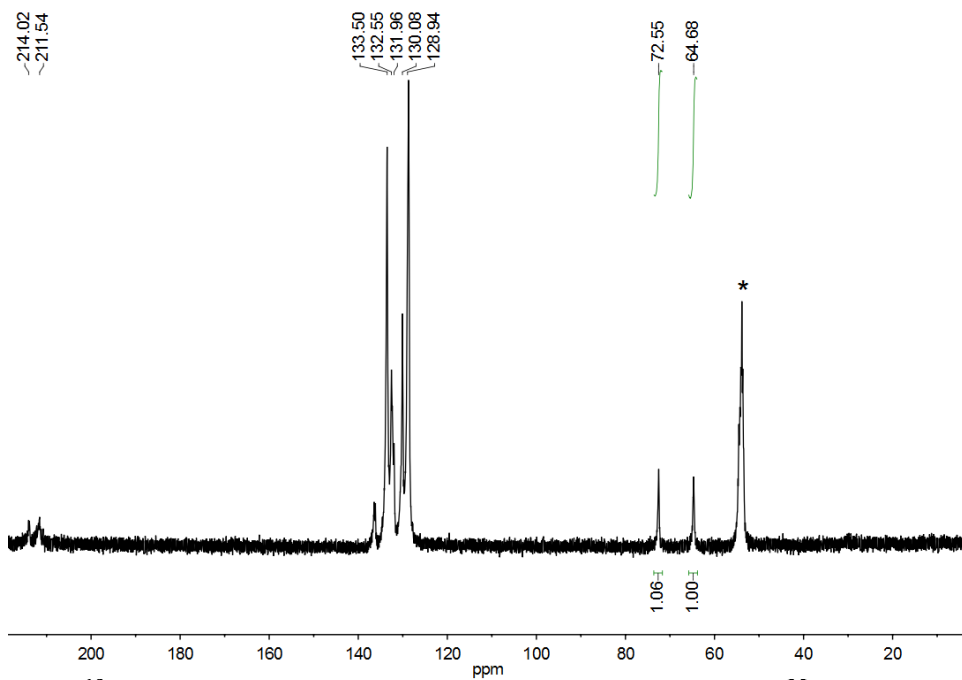


Figure S14. ^{13}C NMR spectrum (125.7 MHz, CD_2Cl_2 solution) of 3^{Me} at 20 °C. Inset: * Residual solvent. Assignments: δ 64.7 (s, 1C, NCH_2Fe), 72.6 (s, 1C, NCH_2S), 129-134 ($\text{P}(\text{C}_6\text{H}_5)_3$).

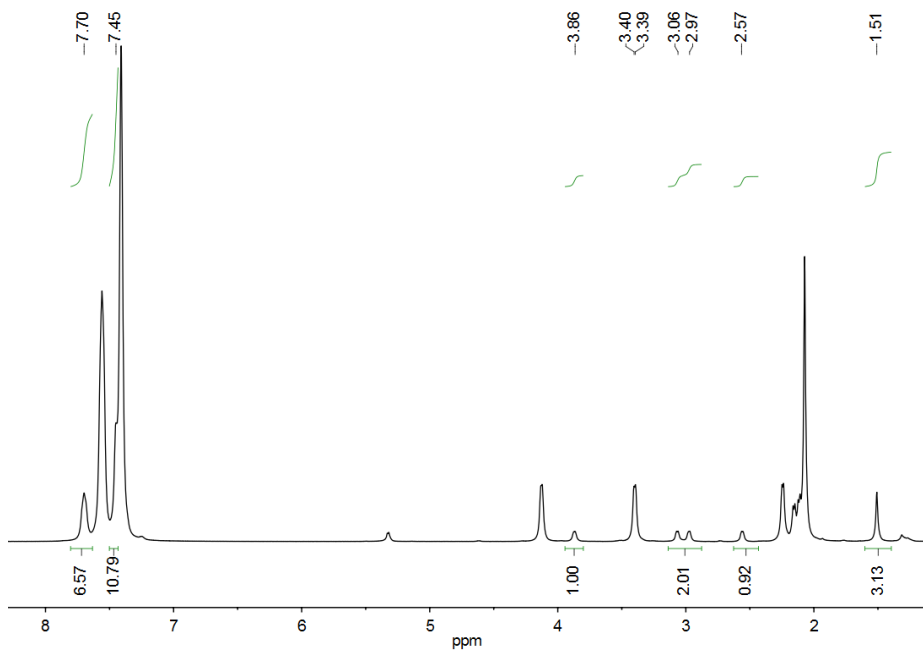


Figure S15. ^1H NMR spectrum of crystals of 3^{Me} (500 MHz, CD_2Cl_2 solution) highlighting minor isomer that forms after 24 h. *Assignments:* δ 1.51 (s, 3H, NCH_3), 2.57 (d, 1H, NCH_2Fe), 2.97 (d, 1H, NCH_2Fe), 3.06 (d, 1H, NCH_2S), 3.86 (d, 1H, NCH_2S), 7.45-7.70 (2s, 15H, $\text{P}(\text{C}_6\text{H}_5)_3$).

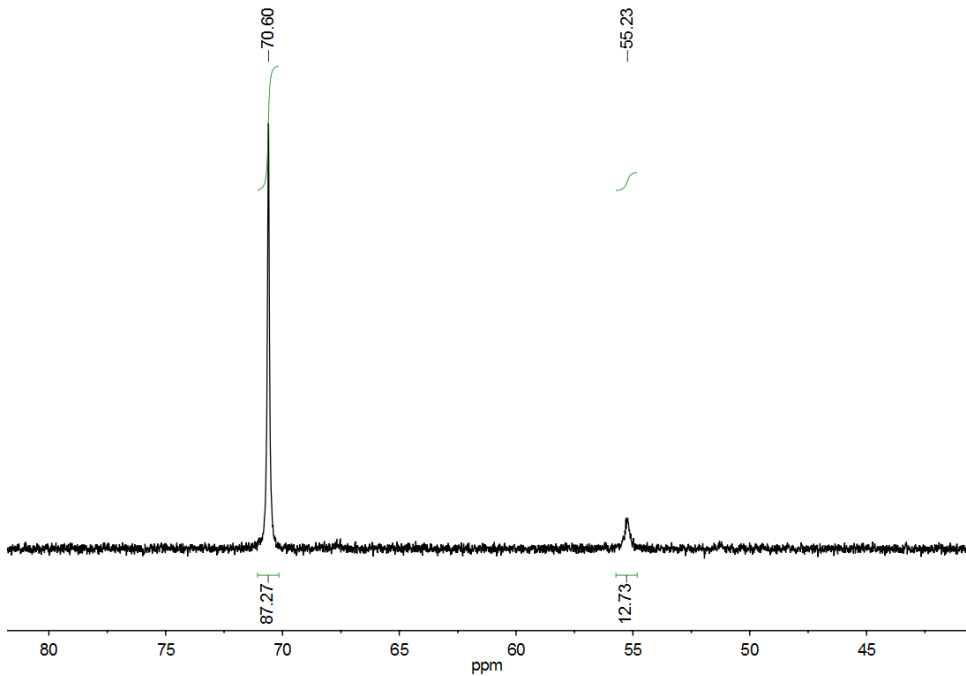


Figure S16. $^{31}\text{P}\{^1\text{H}\}$ NMR spectrum of crystals of 3^{Me} (202.3 MHz, CD_2Cl_2 solution) after 24 h.

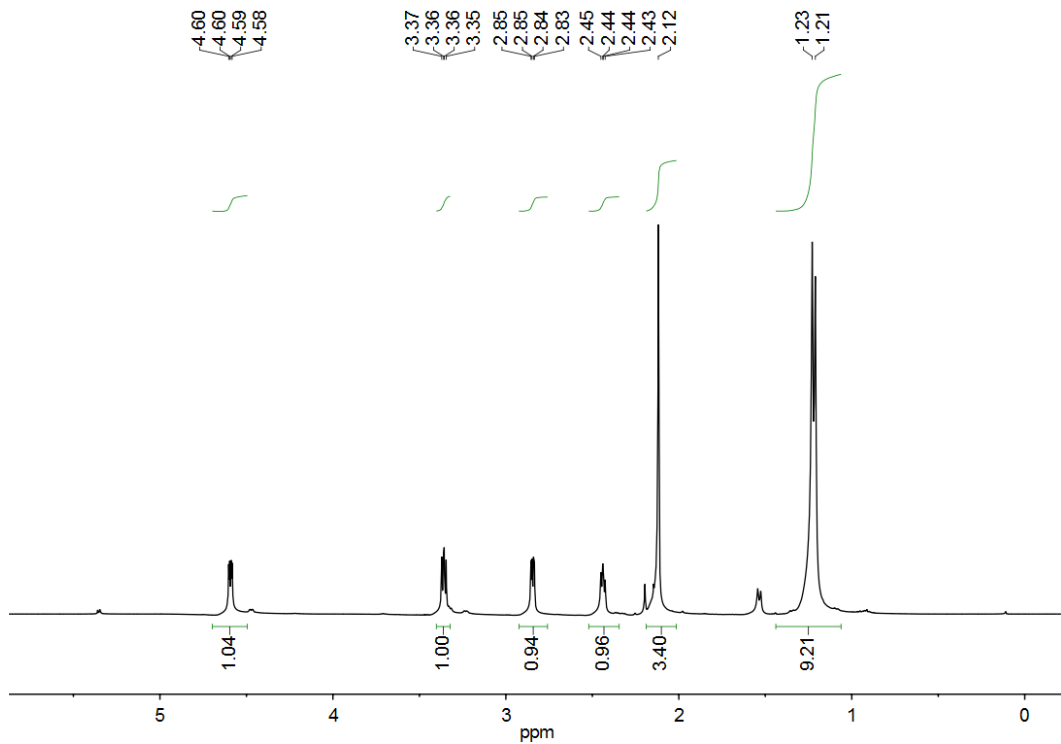


Figure S17. ^1H NMR spectrum (500 MHz, CD_2Cl_2 solution) of 4^{Me} .

Assignments: δ 1.21 (d, 9H, $\text{P}(\text{CH}_3)_3$), 2.12 (2, 3H, NCH_3), 2.44 (d, 1H, NCH_2Fe), 2.85 (dd, 1H, NCH_2Fe), 3.36 (d, 1H, NCH_2S), 4.59 (dd, 1H, NCH_2S).

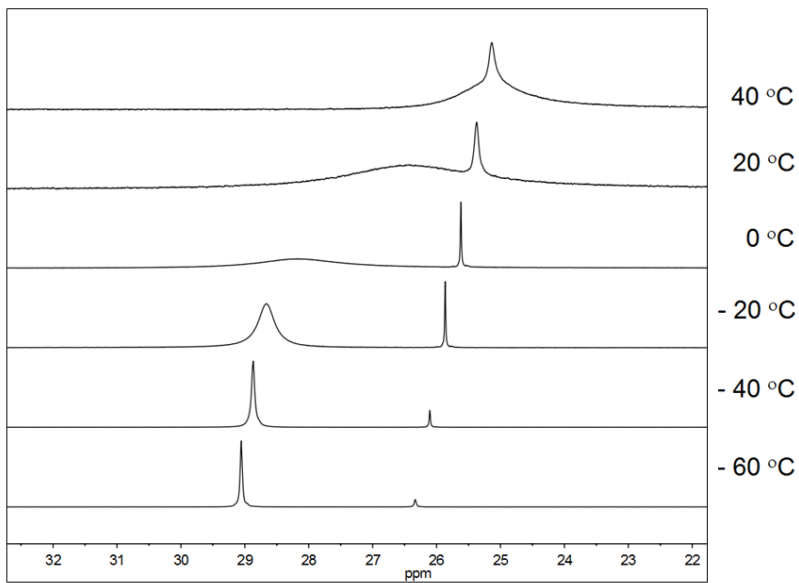


Figure S18. $^{31}\text{P}\{^1\text{H}\}$ NMR spectrum (202.3 MHz, d_8 -toluene solution) of 4^{Me} at various temperatures.

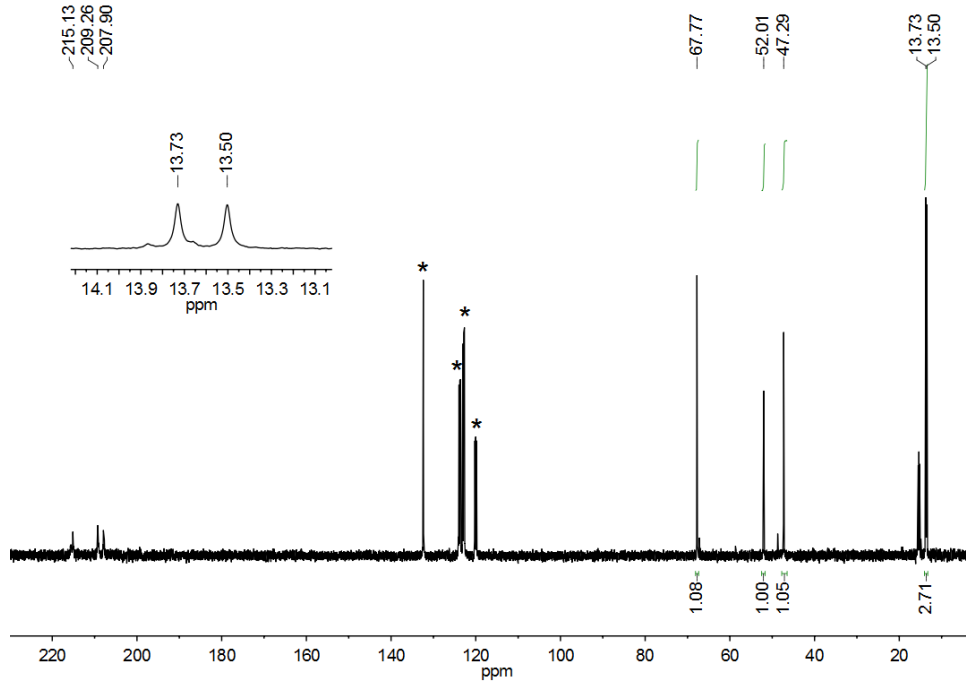


Figure S19. ^{13}C NMR spectrum (125.7 MHz, d_8 -toluene solution) of $\mathbf{4}^{\text{Me}}$ at $20\text{ }^\circ\text{C}$. * Residual solvent. Assignments: δ 13.5 (d, 1C, P(CH₃)₃, $J_{\text{PC}} = 28.9$ Hz), 47.3 (s, 1C, NCH₃), 52.0, (s, 1C, NCH₂Fe), 67.8 (s, 1C, NCH₂S), 208-215 (3s, 3 C, Fe(CO)₃).

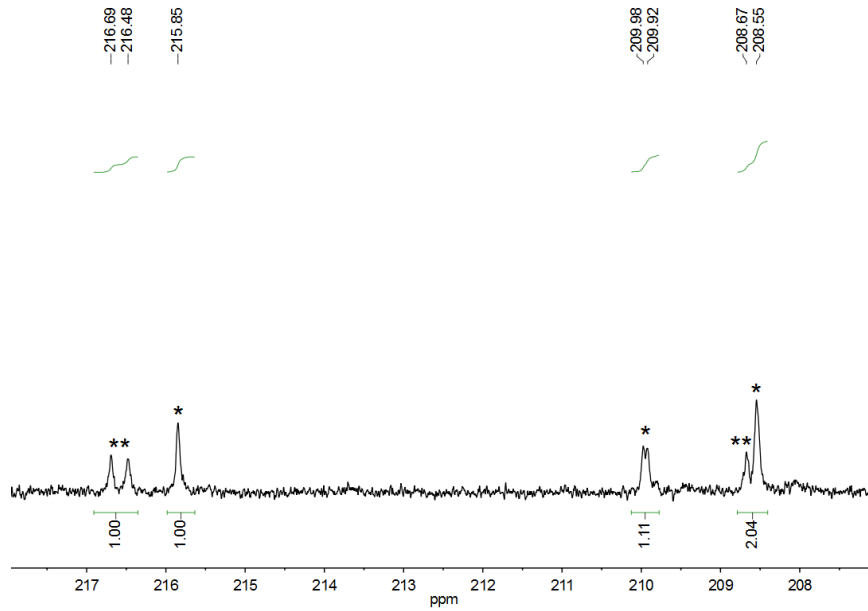


Figure S20. ^{13}C NMR spectrum (125.7 MHz, d_8 -toluene solution) of $\mathbf{4}^{\text{Me}}$ at $-60\text{ }^\circ\text{C}$. * Rigid iron center (3C, Fe^{CH₂}(CO)₃); ** non-rigid iron center (2C, Fe^{NMe}(CO)₂PM₃).

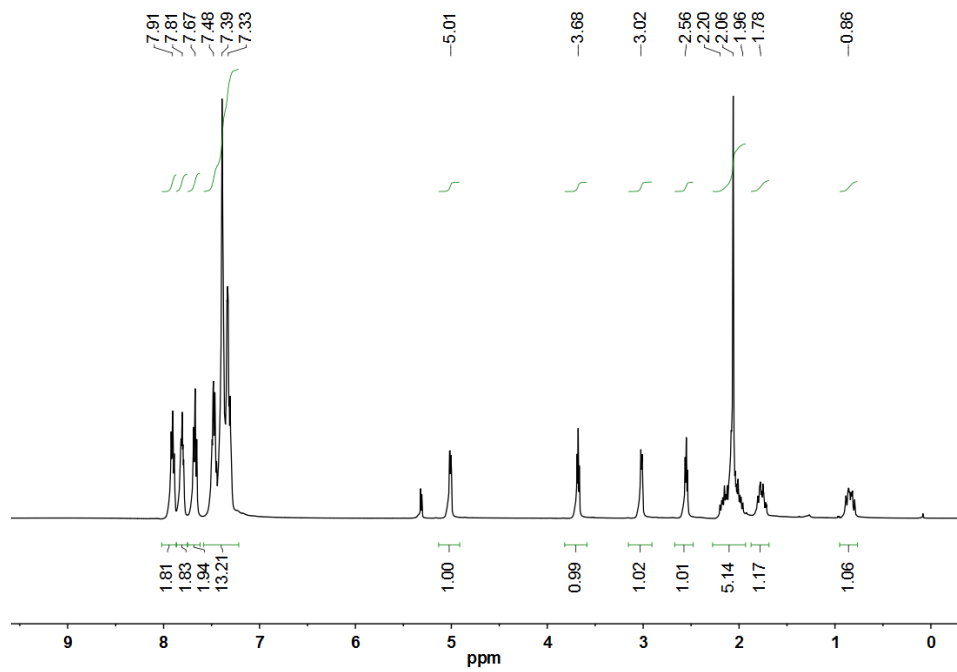


Figure S21. ^1H NMR spectrum (500 MHz, CD_2Cl_2 solution) of $\mathbf{5}^{\text{Me}}$.

Assignments: δ 2.06 (s, 3H, NCH_3), 2.56 (dd, 1H, NCH_2Fe), 3.02 (d, 1H, NCH_2Fe), 3.68 (dd, 1H, NCH_2S), 5.01 (d, 1H, NCH_2S), 0.9-2.10 (m, 10H, $\text{PCH}_2\text{CH}_2\text{P}$), 7.37-7.95 (m, 20H, $\text{P}(\text{C}_6\text{H}_5)_2$).

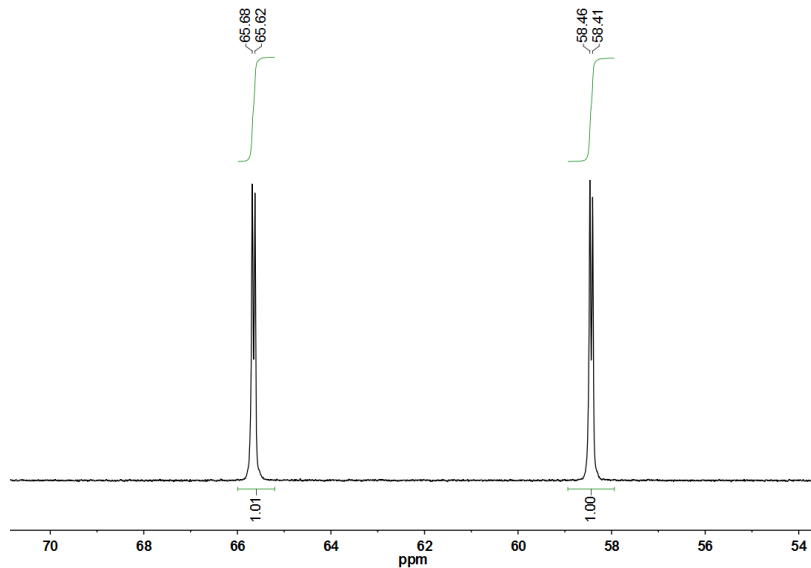


Figure S22. $^{31}\text{P}\{^1\text{H}\}$ NMR spectrum (202.3 MHz, CD_2Cl_2 solution) of $\mathbf{5}^{\text{Me}}$. $J_{\text{PP}} = 11.8$ Hz.

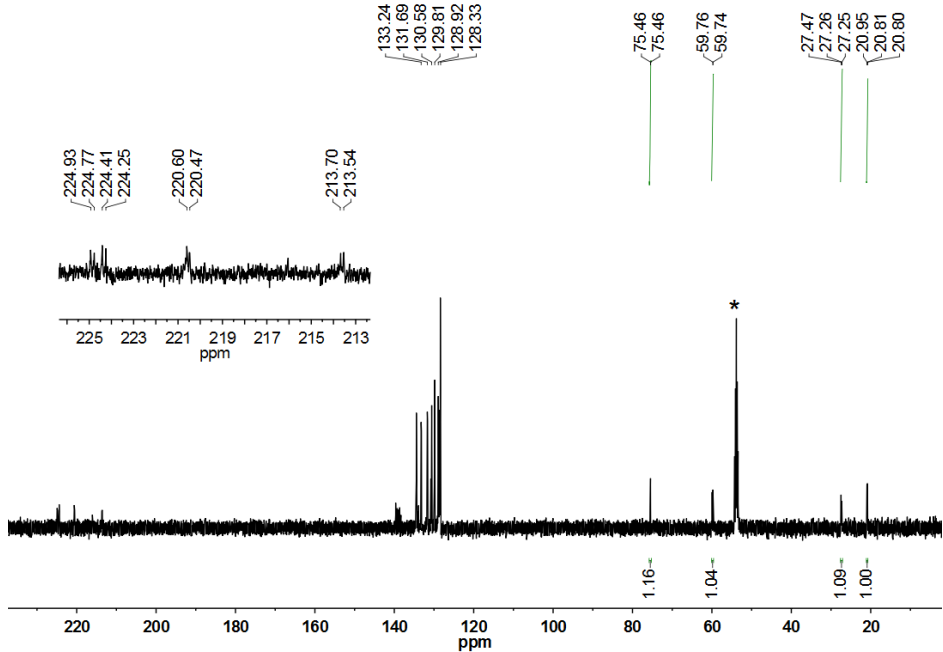


Figure 3. ^{13}C NMR spectrum (125.7 MHz, CD_2Cl_2 solution) of $\mathbf{5}^{\text{Me}}$ at 20 °C. *Residual solvent. Assignments: δ 20.8 (t, 1C, $\text{PCH}_2\text{CH}_2\text{P}$), 27.3 (t, 1C, $\text{PCH}_2\text{CH}_2\text{P}$), 560 (d, 1C, NCH_2Fe), 75.5 (d, 1C, NCH_2S), 128.33-133.24 (m, 24 C, $\text{P}(\text{C}_6\text{H}_5)_2$), 214-225 (4d, 4C, $\text{Fe}(\text{CO})_2$).